Comparative Metabolomic and Network Analysis of the Hyperaccumulation of Astaxanthin in *Haematococcus pluvialis* under the Different Stress Conditions

Yong Dou , Jiayi Li , Zhiyi Qiao * , Wenli Zhou *

Posted Date: 31 October 2023

doi: 10.20944/preprints202310.2052.v1

Keywords: Haematococcus pluvialis; Astaxanthin; Environmental stress factors; Metabolomic analysis; Metabolic network

Article

Comparative Metabolomic and Network Analysis of the Hyperaccumulation of Astaxanthin in *Haematococcus pluvialis* under the Different Stress Conditions

Yong Dou [1,2,3], Jiayi Li [3] and Zhiyi Qiao [1,3,*],Wenli Zhou [1,3,*]

[1] Key Laboratory of Smart Breeding (Co-construction by Ministry and Province), Ministry of Agriculture and Rural Affairs）, Tianjin Agricultural University, 300384, Tianjin, P.R.China
[2] Tianjin Key Laboratory for Green and Ecological Forage, Tianjin Modern Tianjiao Agricultural Technology Co.,Ltd, 301800, Tianjin, P.R.China
[3] Tianjin Key Lab for Aquaculture Ecology and Cultivation, Tianjin Agricultural University, 300384, Tianjin, P.R.China
* Correspondence: zhiyiqiao@tjau.edu.cn, wlzhou69@126.com

Simple Summary: *Haematococcus pluvialis* is a type of excellent bioreactor for astaxanthin production. So far, although a series of measures has been used to induce astaxanthin accumulation in *H. pluvialis*, the mechanisms of the effects varied greatly. Therefore, revealing the common metabolic pathways behind the different induce measures was a very important issue. In the present study, we analyzed the metabolites profile and crucial metabolic pathways related to the astaxanthin accumulation in *H. pluvialis* under the high salinity and nitrogen deficient conditions, using the comparative metabolomic method. It was found that the various effects of the different stress factors on astaxanthin accumulation *in H. pluvialis* existed, while the metabolic networks were constucted. Moreover, the major carbon metabolism and the changes in identified metabolites in *H. pluvialis* under the high salinity and nitrogen deficient stress were presented. These findings provided the comparative metabolomic view of astaxanthin accumulation in *H. pluvialis* under the different stress conditions, furthermore showed a novel insights into the astaxanthin production induced by the environmental stress factors.

Abstract: Variation in metabolite profiles of under high salinity and nitrogen constraint conditions are the key issues of study at the present. To investigate the optimum NaCl and $NaNO_3$ concentration and the corresponding metabolic pathways of astaxanthin accumulation in *H. pluvialis*, a 26-day batch culture experiment of *H. pluvialis* treated under the variable concentration gradients of NaCl and $NaNO_3$ were conducted. The results indicated that 7.5g·L^{-1} and nitrogen-deficient were the optimum NaCl and $NaNO_3$ concentration for the astaxanthin accumulation according to single factor experiments respectively, under which the highest contents of astaxanthin accumulated in *H. pluvialis* reached up to 7.51mg·L^{-1} and 5.60mg·L^{-1}. A total of 132 metabolites were analysed using LC-MS/MS technique, among which 30 differential metabolites with statistical significance were highlighted. Subsequently, 18 and 10 differential metabolic pathways in the high salinity and nitrogen-deficient treatments with statistic significance were enriched and annotated respectively. Furthermore, the metabolic networks related to the astaxanthin accumulation were constucted based on the crucial pathways and metabolites. Moreover, the major carbon metabolism in *H. pluvialis* under the high salinity and nitrogen deficient stress were presented, which exhibited the characteristics in the identified metabolites changes under the different stress conditions. The results did not only demonstrate the differential metabolic networks and the distinct changes in the metabolites involved in the major carbon metabolism, related to the astaxanthin accumulation *in H. pluvialis* under the different stress factors, but provided the regulation targets for astaxanthin production in practice.

Keywords: *Haematococcus pluvialis*; Astaxanthin; Environmental stress factors; Metabolomic analysis; Metabolic network

 doi:10.20944/preprints202310.2052.v1

1. Introduction

Astaxanthin ($C_{40}H_{52}O_4$) is a ketocarotenoid belonging to the terpene compounds, which is recognized as one of the most powerful antioxidants in nature [1]. The ability to neutralize free radicals and scavenge singlet oxygen of astaxanthin is much stronger than a range of common antioxidants such as zeaxanthin, lycopene, β-carotene or vitamin E [2]. Moreover, excellent biosafety properties of natural astaxanthin has been confirmed, which made it apply to health products, dietory supplements and aquaculture. According to the recent research, astaxanthin has been showed obviously beneficial effects on human health and used to the adjuvant treatment for a range of diseases, such as cataract, atherosclerosis and cardiovascular disease [3]. In the field of aquaculture, astaxanthin has been widely used as the colorant and immunopotentiator, which maintained body color of ornamental fish, and provided immune enhancement ability for aquaculture economic animals. Given the excellent biological activity and a wide range of applications, the astaxanthin market will be estimated up to $2.57 billion by 2025 [4].

Haematococcus pluvialis is a type of unicellular green algae, which is distributed in variable freshwater, saline and semi-saline habitats worldwide [5-9]. Furthermore, *H. pluvialis* is widely recognized as one of the best natural sources of astaxanthin. Under the stressed conditions, the planktonic cells of *H. pluvialis* gradually lose their flagella and then formed immotile spores, in which astaxanthin would be generated and accumulated up to 4.0% of the dry weight [10-12]. Moreover, variable strategies to accelerate the astaxanthin accumulation in *H. pluvialis* have been conducted, contained regulation of the environmental stress factors, artificial mutation breeding, external carbon source or nutrient enrichment, and induction of exogenous stimuli [13-16].

Genomics, transcriptomics and metabolomics techniques have been well proved to be the effective approach to analyse the biosynthesis mechanism of the secondary metabolites in *H. pluvialis* [17-20]. However, metabolomics is considered to be the most reflective analysis method for the physiology of organisms among all the "omics" techniques, because metabolites are the terminal products after a series of complex physiological metabolic processes. Currently, nuclear magnetic resonance (NMR), mass spectrometry (MS), chromatography spectroscopy (GC), GC-MS and LC-MS techniques have been used to metabolomics study [21-23]. Thus, a series of research results related to a global insight into the regulation networks involved in the secondary metabolites such as β-carotene, astaxanthin and lipids in *H. pluvialis* has been showed [24-26].

In this study, the optimum NaCl and $NaNO_3$ concentrations for the astaxanthin accumulation in *H. pluvialis* were determined, and then under which the content of intracellular astaxanthin were measured. Subsequently, the metabolomics analysis using LC-MS/MS technique and enrichment analysis based on KEGG database were conducted. Furthermore, the differential metabolic patterns induced by high salinity and nitrogen deficiency were interpreted. The results provided the comparative metabolomic view of astaxanthin accumulation in *H. pluvialis* under the different stress conditions, moreover showed a novel insights into the astaxanthin production induced by the environmental stress factors.

2. Materials and Methods

2.1. Experimental Material and Treatment

H. pluvialis was provided by Tianjin Key Lab for Aquaculture Ecology and Cultivation. The microalgal was cultivated in BBM medium at 22±1°C in a light incubator with light intensity of 55μmol/(m^2·s) and light-dark cycle of 12hL: 12hD. During the culture period, the flasks were shaken six times each day to avoid microalgal cells to attach to the walls or sink. *H. pluvialis* in the exponential growth stage were used for the experiments.

75mL cultures of H. pluvialis in the exponential growth stage (ca. 5×10^5 cells·mL-1) was subcultured into 250-mL conical flasks containing 75mL medium. According to the Table 1., the control group and stress treatment groups were arranged in the experiment. Parallel triplicates were set for each experimental group. As the accumulation of astaxanthin in *H. pluvialis* was observed obviously from the 12th day, thus the measurement of astaxanthin was carried out every 2 days from

 doi:10.20944/preprints202310.2052.v1

the 12th day to the 26th day throughout the experiment. The high salinity and low nitrogen treatment groups in which the content of intracellular astaxanthin reached the highest level, compared with any other treatment group, were named as group HS and group LN respectively. In addition, the control group was abbreviated as group CK. Subsequently, the microalgae suspension on the day when the intracellular astaxanthin reached the highest level, from the group CK, group HS and group LN, were sampled to execute metabolomics analysis.

Table 1. Conditions used for accumulation of astaxanthin in *H. pluvialis*.

	Medium	NaCl gradient (g·L^{-1})	$NaNO_3$ gradient (g·L^{-1})
Control	BBM	0.025	0.25
High salinity	BBM	5, 7.5, 10, 12.5	0.25
Low nitrogen	nitrogen-deficient BBM	0.025	0, 0.032, 0.065, 0.13

2.2. Determination of Astaxanthin in H. pluvialis

Astaxanthin in *H. pluvialis* was extracted and analyzed in the light of the experimental procedure of Boussiba et al.[27]. Firstly, microalgal cells were collected and treated with 5% KOH solution in 30% methanol in order to eliminate the interference of chlorophyll. Subsequently, astaxanthin was extracted by dimethylsulfoxide (DMSO) repeatedly until the precipitation turned into colourless. Finally, the absorbance of extracts was measured at 490 nm using a spectrophotometer. The blank contained DMSO only.

2.3. Metabolite Extraction and LC-MS/MS-based Metabolomic Analysis

Sixty milligrams of microalgal samples were thawed at 4°C and 100μL aliquots were mixed with 400μL pre-cooled methanol/acetonitrile (1:1, v/v) to eliminate the protein. And then the mixture was collected and centrifuged for 20 min (14000r·min^{-1}, 4°C). Furthermore, the samples were re-dissolved in 100μL acetonitrile/water (1:1, v/v) and fully shaked, and then centrifuged for 15min (14000r·min^{-1}, 4°C). The supernatants were collected to conduct the LC-MS/MS analysis.

For HILIC separation, all the samples were detected using a ACQUIY UPLC BEH column. In both ESI positive and negative modes, the mobile phase contained A and B. A was a mixed solution of ammonium acetate and ammonium hydroxide with the concentration of 25 mmol·L^{-1} respectively, and B was a acetonitrile solution. For RPLC separation, a ACQUIY UPLC HSS T3 column was used. In ESI positive mode, the mobile phase contained A and B. A was a solution with 0.1% formic acid dissolved in water, and B was a solution of acetonitrile mixed with 0.1% formic acid. While in ESI negative mode, the mobile phase included A and B. A was a solution of 0.5 mmol·L^{-1} ammonium fluoride dissolved in water, and B was a solution of acetonitrile. The ESI source parameters were made the following settings: Ion Source Gas1 and Gas2 as 60 respectively, curtain gas (CUR) as 30, source temperature as 600°C, IonSpray Voltage Floating (ISVF) as ± 5500 V.

2.4. Data Process and Analysis

Extraction of raw MRM data for all the metabolites was conducted, and then the raw data was conversed to netCDF format. Subsequently, the data with netCDF format was imported to XCMS based on R 3.5.2 software, and the data extraction, peak matching, baseline correction and filling gaps were conducted, therefore a file containing information such as retention time, charge-to-mass ratio and peak area that can be used for subsequent data analysis was obtained. In addition, one-way ANOVA was used to analyze the differences among the metabolites. Moreover the metabolites with $P<0.05$ and fold change≥1.5 were defined as the differential metabolites with statistical significance among the CK, HS and LN group.

Principal component analysis (PCA), a multivariate statistical analysis method, was used to judge the differences among the samples belonging to the variable treatments through R 3.5.2

Preprints (www.preprints.org) | NOT PEER-REVIEWED | Posted: 31 October 2023 doi:10.20944/preprints202310.2052.v1

software. And then the hierarchical clustering was conducted based on the euclidean distance algorithm. Furthermore, the heatmap of hierarchical clustering was obtained with the aim to visualize the differential metabolites. KEGG (Kyoto Encyclopedia of Genes and Genomes) is the major public database related to the pathways in the organism, which contains a series of genes and metabolites information. The metabolites detected in this study were mapped to KEGG metabolic pathways for pathway analysis and enrichment analysis, then the enriched metabolic pathways and signal transduction pathways were identified significantly in differential metabolites by pathway enrichment analysis, compared with the whole background [28].

The metabolic networks were constructed using the Advanced Network Graph Online Tools on the GENE DENOVO website (http://www.omicshare.com). In the network gragh, the metabolic pathways and the differential metabolites were represented using the green filled circles and the pink filled circles respectively, and the quatity of metabolites enriched in the specific pathway was reflected by the size of the green circle. Otherwise, the associated pathways and metabolites were linked up by the black solid lines, which exhibited the regulatory relationship among the metabolic pathways and the metabolites.

The contents of astaxanthin in the different treatments on the each sampling time were analyzed using one-way ANOVA (One-way Analysis of Variance) and Duncan's multiple comparison based on the software SPSS 22.0. The significant level was set at P=0.05.

3. Results

3.1. Effect of NaCl Concentration on Astaxanthin Accumulation in H. pluvialis

The level of astaxanthin in *H. pluvialis* raised gradually, and then tended to keep steady under the high salinity stress during the experiment. The contents of astaxanthin in 5, 7.5 and 10g·L^{-1} treatment groups were higher than the CK group significantly (P<0.05), while which in 12.5g·L^{-1} treatment group was insignificant compared with the CK group (P>0.05). According to the Figure 1., the level of astaxanthin accumulated in *H. pluvialis*, in 7.5g·L^{-1} NaCl group, was higher than any other groups roughly thoughout the experiment (P<0.05), furthermore in which the highest level of astaxanthin reached up to 7.51mg·L^{-1} on the 24th day. However, the excessive NaCl concentration (12.5g·L^{-1}) was not beneficial to the accumlation of astaxanthin in *H. pluvialis*. This result indicated that there was a certain NaCl concentration threshold, above or below which the level of astaxanthin accumulated in *H. pluvialis* would drop.

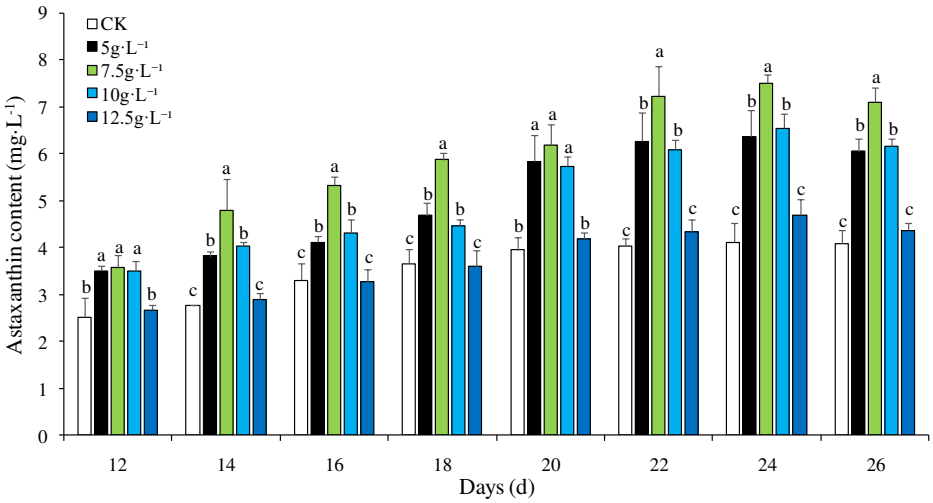

Figure 1. Effect of NaCl concentration on astaxanthin accumulation in *H. pluvialis*. Note: The treatments with the same letter showed insignificant at the level 0.05 (P>0.05), while the ones with the different letter showed significant at the level 0.05 (P<0.05).

Preprints (www.preprints.org) | NOT PEER-REVIEWED | Posted: 31 October 2023 doi:10.20944/preprints202310.2052.v1

3.2. Effect of $NaNO_3$ Concentration on Astaxanthin Accumulation in H. pluvialis

The concentration of astaxanthin in *H. pluvialis* increasd gradually, and then reduced slowly under the nitrogen limitation stress during the experiment. According to the Figure 2., the content of astaxanthin was the highest among the treatment groups under the nitrogen-deficient stress ($0g \cdot L^{-1}$) thoughout the experiment ($P<0.05$), while those of 0.032、0.065 and $0.13g \cdot L^{-1}$ treatment groups were insignificant compared with the CK group ($P>0.05$). The astaxanthin accumulation in *H. pluvialis* was relatively slower before the 14th day, however the accumulation rate speeded up from the 14th day to the 22th day. The astaxanthin content in *H. pluvialis* reached up to $5.60mg \cdot L^{-1}$ at the highest level in the nitrogen-deficient group, which was 28% higher than the CK group.

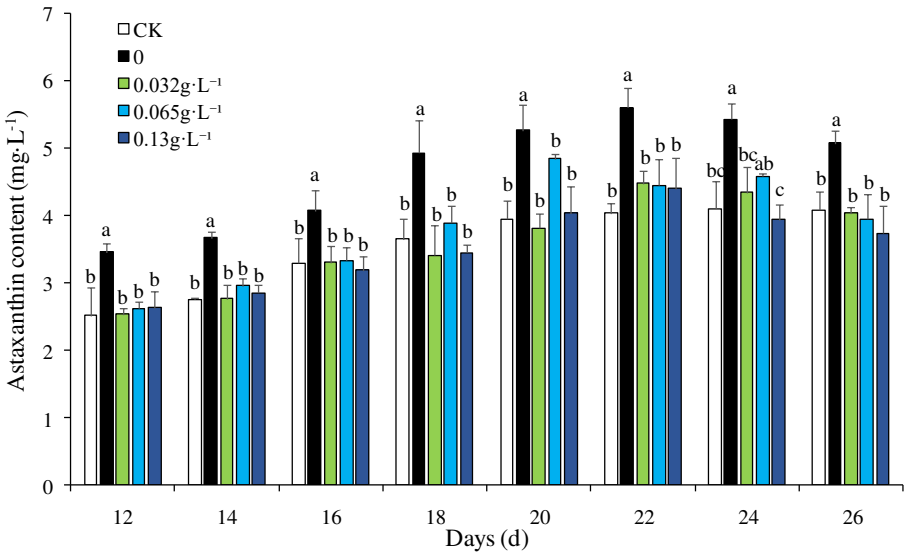

Figure 2. Effect of $NaNO_3$ concentration on astaxanthin accumulation in *H. pluvialis*. Note: The treatments with the same letter showed insignificant at the level 0.05 ($P>0.05$), while the ones with the different letter showed significant at the level 0.05 ($P<0.05$).

3.3. Comparison of the Metabolic Characteristics in H. pluvialis under the Different Stress Conditions

PCA plot of the metabolomic profiles under the different stress conditions was generated, in which the distribution and concentration of each sample was showed clearly. According to the Figure 3., the metabolomic results of the environmental stress treatments and control group among all samples were distinct in the experiment, which suggested that the effects of high salinity and nitrogen-deficient on the global metabolomic profiles related to the astaxanthin accumulation in *H. pluvialis* were differential.

Preprints (www.preprints.org) | NOT PEER-REVIEWED | Posted: 31 October 2023 doi:10.20944/preprints202310.2052.v1

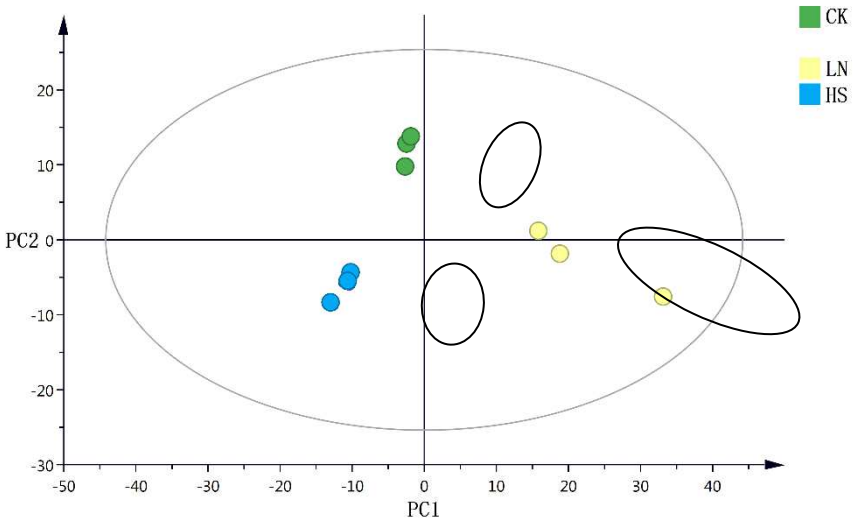

Figure 3. PCA plot of metabolomic profiles.

As shown in Table 2., a total of 132 metabolites in *H. pluvialis*, under the different stress conditions, were identified by LC-MS/MS technigue. In addition, one-way ANOVA was used to analyze the differences among the metabolites. Metabolites with $P<0.05$ and fold change≥1.5 were defined as the differential ones with statistical significance among the CK, HS and LN group. And then the heatmap of hierarchical clustering was obtained with the aim to visualize the differential metabolites (Figure 4.).

Table 2. Metabolites profile of H. pluvialis detected using LC-MS/MS technique.

Metabolite	KEGG code	Fold change		Metabolite	KEGG code	Fold change	
		[illegible]S vs CK	[illegible]N vs CK			[illegible]S vs CK	[illegible]N vs CK
N2,N2-Dimethylguanosine	NA	0.35	0.33	5-Hydroxynicotinic acid	C01020	0.81	1.77
AMP	C00020	0.19	0.47	N6-Acetyl-L-lysine	C02727	0.72	0.42
Glycerophosphocholine	C00670	0.73	0.57	ATP	C00002	5.11	1.48
Glyceric acid	C00258	0.35	0.23	L-Lactic acid	C01432	0.85	0.47
5-hydroxy-Tryptophan	C01017	0.15	0.46	NAD	C00003	1.32	0.36
Nicotinic acid	C00253	0.43	0.48	N-Acetyl-D-glucosamine	C00140	0.97	0.49
L-Aspartate	C00049	4.14	2.42	NAAD	C00857	1.30	0.35
L-Proline	C00148	0.85	0.52	N-Acetylcadaverine	NA	1.85	0.69
Thymine	C00178	4.62	2.11	dAMP	C00360	0.34	0.76
L-Carnitine	C00318	0.39	0.84	Malate	C00711	0.92	0.34
UMP	C00105	0.31	0.41	N-Carbamoyl-L-aspartic acid	C00438	1.99	0.63
cAMP	C00575	0.40	0.21	Guanosine	C00387	1.75	0.38
γ-Glutamyl-L-methionine	NA	3.09	1.17	L-Asparagine	C00152	0.96	0.56
GDP	C00035	1.99	3.12	Cytidine	C00475	0.72	0.75
Nicotinamide	C00153	1.80	1.53	Arginine	C03406	0.57	0.25
Dimethylglycine	C01026	0.53	0.97	Sucrose	C00089	1.17	0.53
2'-O-methyladenosine	C04779	0.71	0.35	Orotic acid	C00295	0.26	0.67
γ -L-Glutamyl-L-phenylalanine	NA	1.00	8.80	Allantoic acid	C00499	0.31	0.50
5'-Deoxyadenosine	C05198	0.78	0.06	L-Citrulline	C00327	2.35	0.52
5-Aminopentanoic acid	C00431	0.58	0.68	Flavone	C15608	0.46	1.23
L-Tyrosine	C00082	4.51	0.80	7-methylguanosine	NA	1.13	0.39
Pantothenic acid	C00864	0.88	0.44	Riboflavin	C00255	0.72	1.12
L-Pipecolic acid	C00408	2.92	1.44	FAD	C00016	1.24	0.45
Deoxycytidine	C00881	1.50	2.15	cis-4-Hydroxy-D-proline	C03440	0.20	0.08
N-Acetylglutamine	NA	1.97	1.42	NADP	C00006	4.32	0.54

Preprints (www.preprints.org) | NOT PEER-REVIEWED | Posted: 31 October 2023 doi:10.20944/preprints202310.2052.v1

CMP	C00055	0.63	0.43	Biopterin	C06313	0.36	1.29
Tryptamine	C00398	0.51	0.42	L-Glutamate	C00025	1.05	0.40
Choline	C00114	0.50	1.03	L-Homoserine	C00263	1.19	0.60
CDPcholine	C00307	0.49	0.38	Hypoxanthine	C00262	0.46	1.30
Glycerol3P	C00093	0.37	0.38	Pyridoxal	C00250	1.06	0.70
cis-Aconitate	C00417	1.97	2.78	2,3-Dihydroxybenzoic acid	C00196	1.34	0.25
Nicotinamide ribotide	C00455	3.47	3.62	Cholesterol sulfate	C18043	1.39	1.56
Adenine	C00147	0.99	3.87	N-Formylmethionine	C03145	1.62	0.18
N-Acetyl-L-alanine	NA	0.38	0.31	Glycyl-L-leucine	C02155	0.62	1.11
Xanthosine	C01762	0.51	0.36	L-Valine	C00183	1.32	0.46
Deoxyguanosine	C00330	2.02	0.83	4-Guanidinobutyric acid	C01035	0.70	0.94
D-Neopterin	C05926	2.44	0.37	FMN	C00061	1.60	0.94
Succinate	C00042	0.66	0.31	Glutathione disulfide	C00127	1.85	0.66
O-Succinyl-L-homoserine	C01118	0.58	0.09	Urocanic acid	C00785	0.59	0.59
Uric acid	C00366	1.18	1.41	L-Methionine	C00073	1.39	0.23
N6-methyladenosine	NA	0.75	0.24	2-keto-D-Gluconic acid	C06473	1.33	0.29
D-glucosamine 1-phosphate	C06156	0.48	0.32	L-Homocysteic acid	C16511	1.18	0.64
Isobutyryl-CoA	C00630	7.57	0.92	dTMP	C00364	0.56	1.20
DHAP	C00111	0.31	0.26	Inosine	C00294	1.01	0.25
Thiamine	C00378	14.25	101.38	L-Serine	C00065	1.23	0.40
GABA	C00334	1.84	1.16	IMP	C00130	0.30	2.96
GDP-L-fucose	C00325	0.50	0.28	L-2-Aminoadipic acid	C00956	1.13	0.78
Phenyllactic acid	C05607	3.24	0.62	dGMP	C00362	0.42	2.51
D-Glucose-6-phosphate	C00092	0.77	0.42	S-Adenosylhomocysteine	C00021	1.09	0.11
Glycine	C00037	2.16	0.41	N4-Acetylcytidine	NA	0.51	1.81
Creatine	C00300	1.26	1.12	UDP-D-Glucuronate	C00167	2.13	0.27
1-Methylxanthine	C16358	0.61	0.16	UDP -Glucose	C00029	1.70	0.90
Deoxyinosine	C05512	1.64	0.73	L-Kynurenine	C00328	0.97	0.37
Dephospho-CoA	C00882	22.19	1.84	N-Acetyl-L-phenylalanine	C03519	1.44	0.35
β-Hydroxybutyric acid	C01089	1.65	0.46	L-Leucine	C00123	0.64	0.52
TPP	C00068	4.57	1.54	L-Phenylalanine	C00079	0.95	0.65
γ -L-Glutamyl-L-valine	NA	0.82	2.99	taurine	C00245	1.13	0.24
Adenosine	C00212	1.13	0.33	Acetyl-DL-Leucine	NA	1.23	0.37
Phosphoenolpyruvate	C00074	0.77	0.35	dCMP	C00239	0.44	1.32
L-2-Hydroxygluterate	C03196	3.10	0.27	Pyridoxine	C00314	0.86	1.14
Kynurenic acid	C01717	0.51	0.07	L-Tryptophan	C00078	0.96	0.45
L-Glutamine	C00064	0.95	0.98	4-Pyridoxic acid	C00847	0.52	1.71
Pseudouridine	C02067	0.51	1.11	Inositol	C00137	1.33	0.37
L-Lysine	C00047	0.67	0.97	Uridine	C00299	0.94	0.88
Cytosine	C00380	0.57	0.79	Ureidopropionic acid	C02642	0.76	0.15
5-Aminolevulinic acid	C00430	6.15	0.60	Fumarate	C00122	0.96	0.47

According to the judging criteria, a total of 30 differential metabolites containing 3 fatty acids and intermediates, 6 amino acids and derivatives, 1 carbohydrates, 12 nucleoside derivatives and 8 other metabolites were identified and clustered among the CK, HS and LN group. The results showed distinct downregulation of 18 metabolites in the environmental stress treatments, compared with the CK group. Especially, the levels of 3 fatty acids and intermediates, including Glycerol3P, Glyceric acid and Glycerophosphocholine, were much lower than the CK Group. Moreover the downregulation of the intermediate products of nucleotides metabolism such as AMP, UMP and 5'-Deoxyadenosine in the stress treatments was observed. However, 8 metabolites including L-Aspartic Acid, Thymine, Glycine, Guanosine, Sucrose, L-Valine, L-2-Hydroxygluterate and L-Citrulline were upregulated in the HS group. Additionally, the significant upregulation of GDP, IMP, N4-Acetylcytidine and 4-Pyridoxic acid was detected in the LN group.

Preprints (www.preprints.org) | NOT PEER-REVIEWED | Posted: 31 October 2023 doi:10.20944/preprints202310.2052.v1

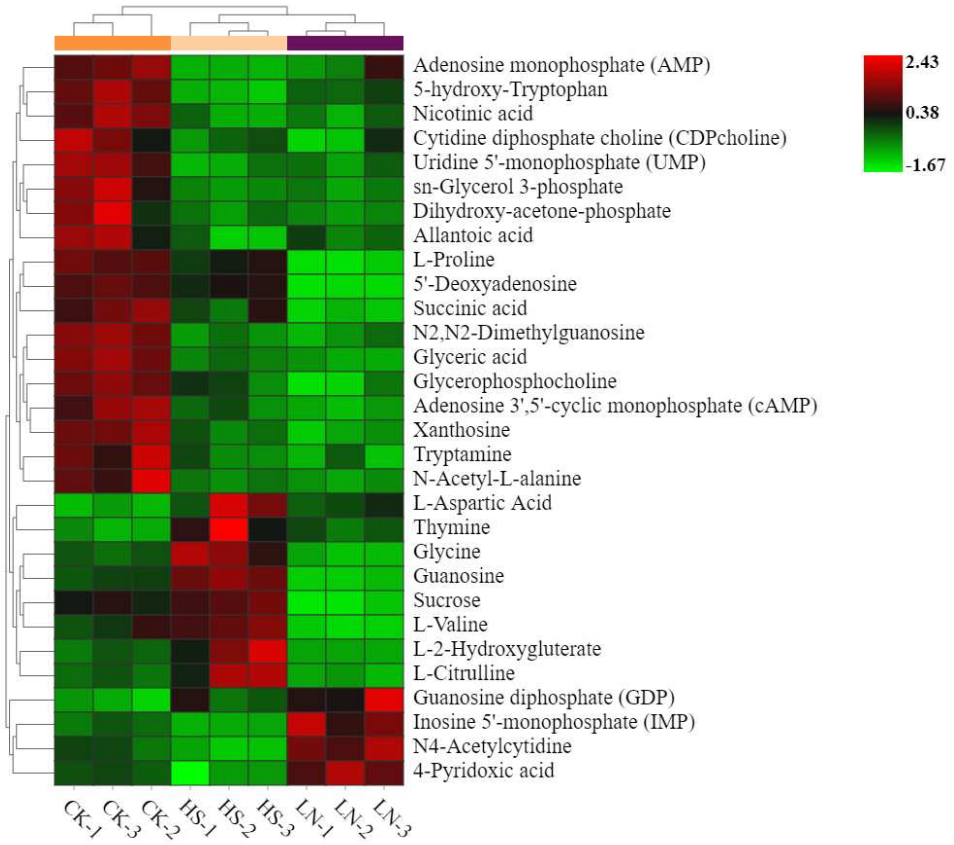

Figure 4. Heatmap of differential metabolomic profiles.

3.4. KEGG Pathway Analysis

To further explore the crucial metabolism pathways related to the accumulation of astaxanthin in *H. pluvialis*, stressed under 7.5g·L^{-1} NaCl, KEGG pathways enrichment analysis was performed for the CK and HS group. 51 differential metabolic pathways were enriched and annotated, among which 18 pathways were statistically significant (P<0.05) (Figure 5.). The results showed that the metabolites involved in key metabolic pathways were regulated and modified under the nitrogen-deficient stress. Furthermore, the significant pathways mainly focused on carbohydrate metabolism, amino acid metabolism and transport, glycerol and derivatives metabolism, nucleotide and derivative metabolism and energy metabolism.

Preprints (www.preprints.org) | NOT PEER-REVIEWED | Posted: 31 October 2023 doi:10.20944/preprints202310.2052.v1

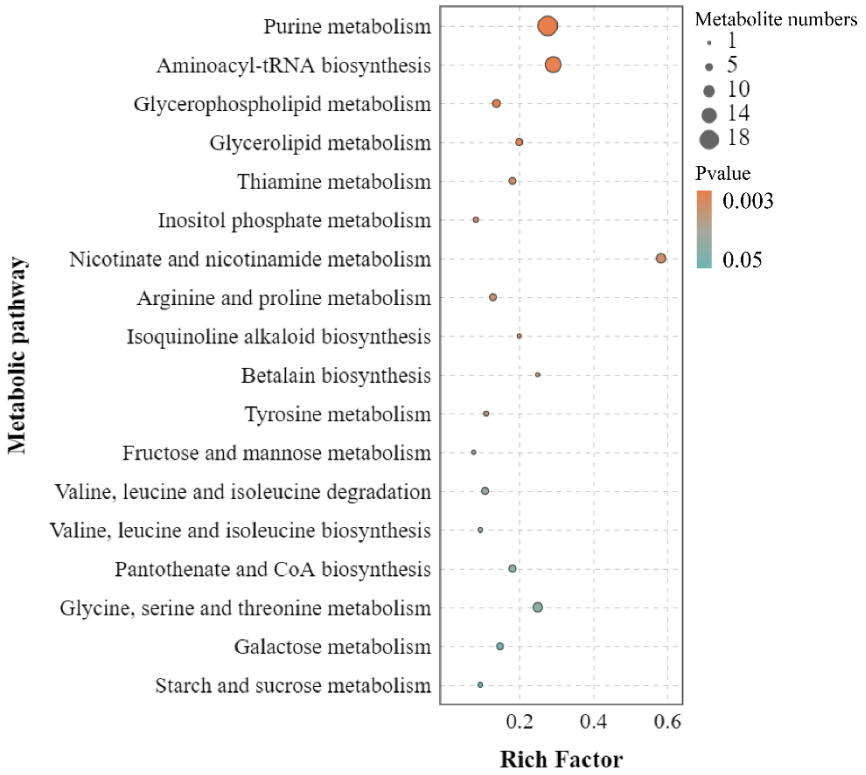

Figure 5. KEGG pathways enrichment analysis between the CK and HS group.

To further reveal the dominant role in the key metabolic pathways related to the astaxanthin accumulation in *H. pluvialis*, under nitrogen-deficient stress, KEGG pathways enrichment analysis was performed for the CK and LN group. 51 differential metabolic pathways were enriched and annotated, among which 10 pathways were statistically significant (P<0.05) (Figure 6.). Moreover, the significant pathways mainly focused on amino acid metabolism and transport, nucleotide and derivative metabolism and energy metabolism.

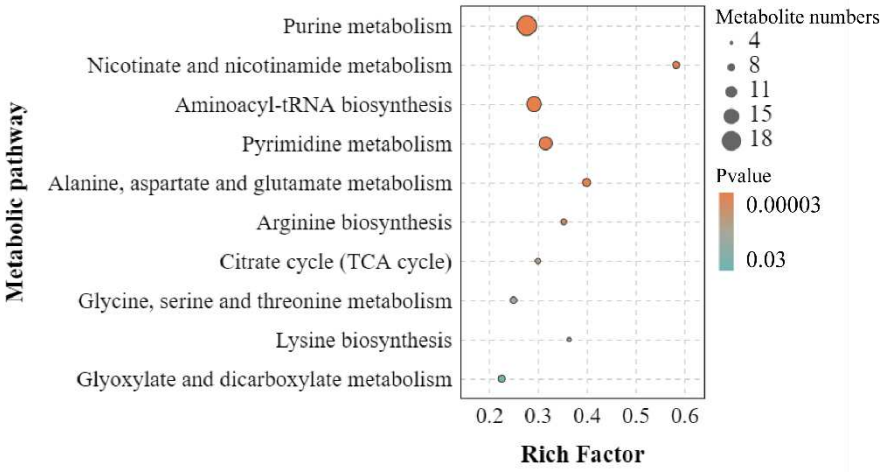

Figure 6. KEGG pathways enrichment analysis between the CK and LN group.

3.5. Metabolimic Network Construction and Analysis

To exhibit the metabolic characteristics related to the astaxanthin accumulation in *H. pluvialis* under the high salinity and nitrogen-deficient conditions respectively, the metabolic networks were constructed based on the crucial pathways and metabolites (Figure 7 and Figure 8.).

Preprints (www.preprints.org) | NOT PEER-REVIEWED | Posted: 31 October 2023 doi:10.20944/preprints202310.2052.v1

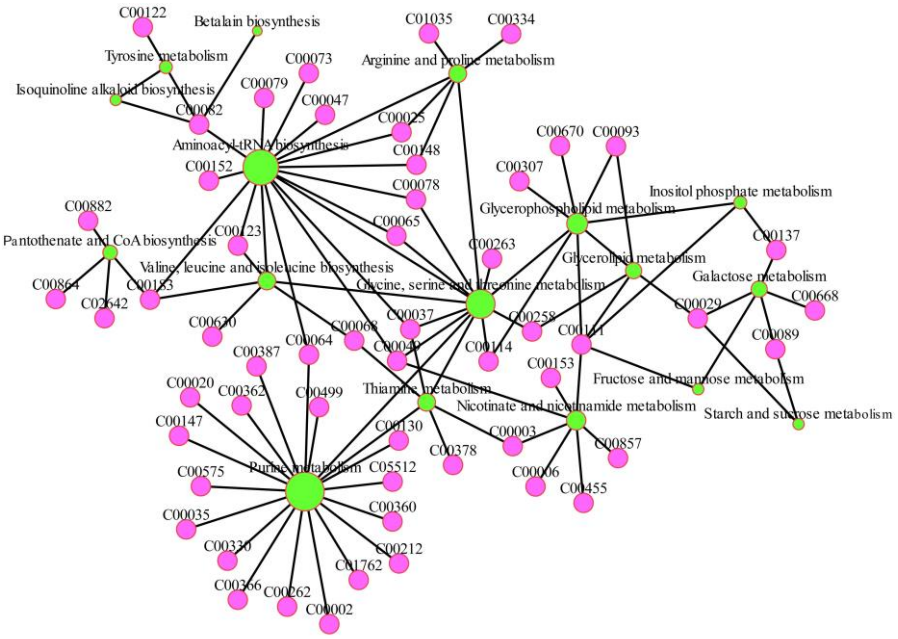

Figure 7. Metabolic network in *H. pluvialis* under the high salinity condition.

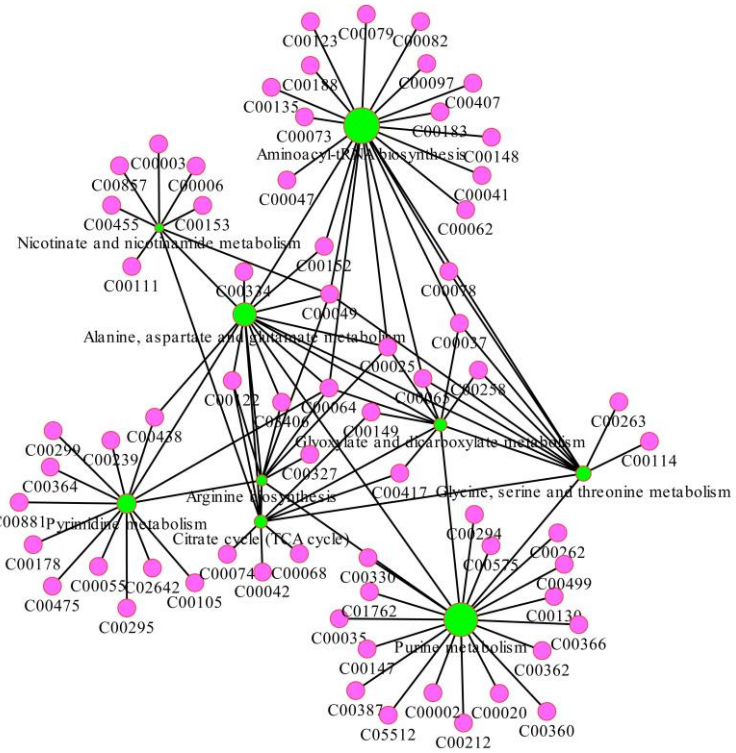

Figure 8. Metabolic network in *H. pluvialis* under the nitrogen-deficient condition.

3.6. Major Carbon Metabolism and the Changes in Identified Metabolites Related to Astaxanthin Accumulation in H. pluvialis

In aims to reveal and compare to the characteristics of the changes in identified metabolites involved in the major carbon metabolism related to the astaxanthin accumulation, under the different environmental stress conditions, the global profiling was exhibited (Figure 9.). The major carbon metabolism contained the carbohydrate and derivatives metabolism, glycerol and derivatives metabolism, amino acid metabolism and energy metabolism. The series of metabolic processes provided not only the precursors and intermediates related to the astaxanthin biosynthesis, but also the energy required in the metabolism scheme. As shown in Figure 9., the contents of the metabolites

Preprints (www.preprints.org) | NOT PEER-REVIEWED | Posted: 31 October 2023 doi:10.20944/preprints202310.2052.v1

in LN group were almost lower than those both in the CK and HS groups, while which in HS group were substantially at the higher or close levels contrast to the CK group. However, the distinct patterns of several metabolites were exhibited according to the gragh. Specially, the content of cis-Aconitate was higher in the LN group than which both in the CK and HS groups. Otherwise, the levels of L-Glutamine in the three groups were almost identical. Moreover, the concentrations of Glycerol3P and DHAP were close to each other in the LN and HS group respectively, while both lower than the CK group. Additionally, the levels of L-Aspartate and GABA increased in order of CK, LN and HS group.

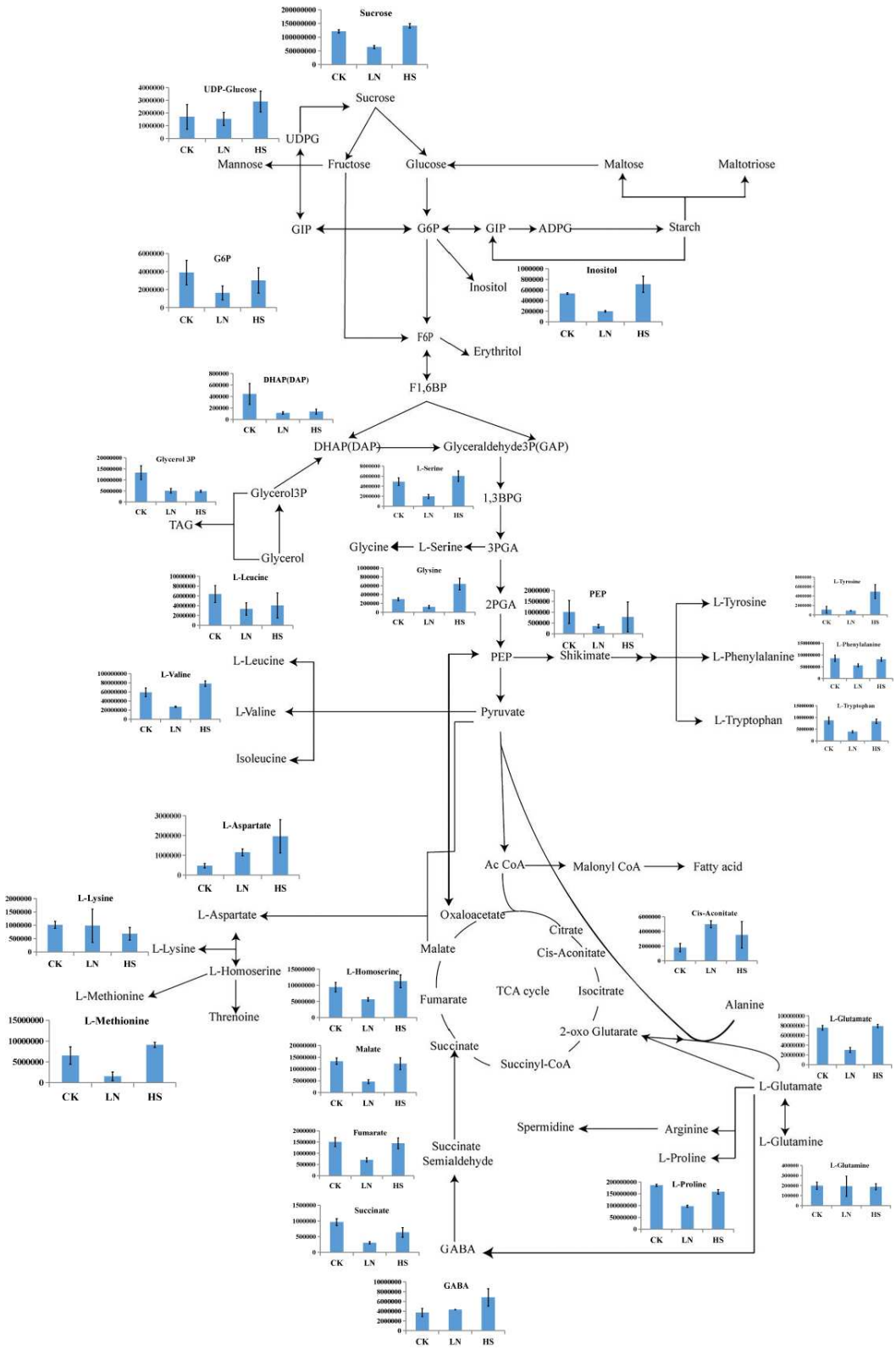

 doi:10.20944/preprints202310.2052.v1

Figure 9. The major carbon metabolism and the changes in identified metabolites in *H. pluvialis* under the different stress conditions. CK represented the control group, while HS and LN represented the high salinity and nitrogen deficient treatments respectively.

4. Discussion

4.1. Metabolic Characteristics of Astaxanthin Accumulation in H. pluvialis under the High Salinity Stress

When the fluctuation of the environmental conditions occurs, the physiological and metabolic processes of microalgae would change obviously. In response to the external environmental stress better, the energy flow and substances synthesis pathways in the cells would be adjusted accordingly. Many organic molecules such as carbohydrates, lipids and pigment synthesized in microalgae have been reported to cope with the variable environmental stress factors. Induced by the environmental stress, the biosynthesis and accumulation of astaxanthin which was the most important substance against stress in immotile cysts of *H. pluvialis* occurred gradually [29-31].

In the present study, the contents of astaxanthin in *H. pluvialis* stressed by the high salinity reached up to 7.51mg·L^{-1}, higher than the CK group significantly(P<0.05). It was highlighted that most of the astaxanthin in *H. pluvialis* did not exist in the free state, but the form of mono- and diesters conmbined with fatty acid (FA) after dehydration. Therefore, the synthesis and accumulation of astaxanthin and FA showed a obvious synchronization [32-33]. This view was proved by the result that upregulation of "glycerophospholipid metabolism" and "glycerolipid metabolism" pathways along with increasing of astaxanthin in the HS group, in the present study. Furthermore, sn-Glycerol-3-phosphate, one of the crucial intermediates of glycerophospholipid metabolism, is a key compound for lipid synthesis, providing the carbon skeleton to formate astaxanthin and lipids in microalgae cells [34]. In this study, the relative contents of sn-glycerol 3-phosphate in *H. pluvialis* were only 36.54% in the HS group of the control group, which suggested the biosynthesis process of astaxanthin was quite active to withstand the high salinity stress condition. In this research, activation of amino acid metabolism is beneficial to astaxanthin accumulation, because amino acid metabolism process can provide the necessary precursors and intermediates for astaxanthin biosynthesis [35]. It was reported that the contents of amino acid, protein and astaxanthin in *H. pluvialis* increased simultaneously under sodium chloride stress condition [36]. However, the metabolic pathways associated with different amino acids showed an obvious complexity in the present study. Specifically, "glycine, serine and threonine metabolism", "valine, leucine and isoleucine biosynthesis" and "tyrosine metabolism" were activated in *H. pluvialis* treated by high salinity stress, leading to significant increase of glycine, L-serine, L-valine and L-tyrosine. This was consistent with the result of previous research [37]. In contrast, "arginine and proline metabolism" was downregulated under the same condition, accompanied with a drop of L-proline. The results implied that the different amino acids maybe play the viarable roles in astaxanthin biosynthesis. Moreover, simultaneous accumulation of GABA and astaxanthin in *H. pluvialis* stressed by the high salinity was observed in the present study, which was demonstrated in several previous studies [38-39]. In microalgae, GABA metabolism plays an important role in the organic acid and amino acid biosynthesis, and GABA is considered as a temporary nitrogen storage under stressful conditions [40]. Therefore, rising GABA would provide more intermediates for astaxanthin accumulation and substance reserves to cope with high salinity stress. As one precursor involved into GABA biosynthesis, glutamate would be transformed into GABA through GAD pathway [36]. In this research, the significantly opposite trends between GABA and glutamate were observed, indicated that the biotransformation of glutamate to GABA was quite active.

Carbohydrates are not only the important energy providers for microalgae, but also the raw materials for many physiological and metabolic process. It was demonstrated that the carbohydrates depletion in microalgae might be promoted because of the secondary metabolites accumulation, containing lipids and astaxanthin, stressed by the abiotic factors [37]. Yet, the level of sucrose in *H. pluviali*, the only carbohydrate detected in the present study, rised in tandem with astaxanthin under high salinity stress. Nevertheless, although "fructose and mannose metabolism" and "starch and

 doi:10.20944/preprints202310.2052.v1

sucrose metabolism" were enriched significantly between the CK and HS group, their involvement in astaxanthin accumulation were limited according to Figure 7. These inconsistent results suggested that the carbohydrate metabolism would be closely related to the strain of microalgal and the specific state of stress, and the raw materials required for astaxanthin synthesis were probably variable in different situations. Maltose would be turned into the carbon skeleton for the biosynthesis of astaxanthin and FA [18]. Although maltose and sucrose are isomers of each other, the interconversion of them in microalgae has not been found. In this research, increasing sucrose content indicated that it has not been consumed appreciably, implying that the biotransformation between sucrose and maltose would not occur in *H. pluvialis*. Additionally, inositol phosphate is an important signal molecule involved in several physiological metabolic processes, while inositol is the product of dephosphorylation of inositol phosphate. The relative content of inositol in the HS group was 1.33-fold of the control, hinting that the inositol phosphate signal transduction system inhibited under high salinity stress.

4.2. Metabolic Characteristics of Astaxanthin Accumulation in H. pluvialis under the Nitrogen-deficient Stress

According to the previous studies, nitrogen-deficient culture was an effective approach to facilitate the astaxanthin accumulation in *H. pluvialis*. However, variation of substance metabolism and flow occurred under the nitrogen-deficient stress condition, compared with the normal status [35, 37, 39]. Furthermore, to cope with the nitrogen constraint stress, resource allocation in cells would be adjusted accordingly. In particular, the processes of carbon metabolism and nitrogen metabolism were reintegrated, not only ensured the nitrogen balance in the cells, but the biosynthesis of anti-stress substances.

Under the nitrogen-deficient condition, proteins, one of the intracellular nitrogen storage, serve as a crucial role in the modulation of nitrogen metabolism, the levels of intracellular amino acids and protein reduced significantly, and nitrogen was perhaps recycled into amino acids synthesis in response to the resource constraints [40]. The proteins related to the catabolism would be re-distributed after the fluctuation of carbon skeletons during the biosynthesis of organic compounds [41]. In this study, "glycine, serine and threonine metabolism" and "arginine biosynthesis" were regulated significantly under the nitrogen-deficient condition. Subsequently, the contents of most amino acids including L-proline, glycine, L-glutamate, L-methionine, L-serine, L-leucine, L-phenylalanine, L-Tyrosine, arginine and L-valine in the LN group decreased significantly, which implied that quite a lot of amino acids in *H. pluvialis* were converted to endogenous nitrogen sources in response to nitrogen limitation. In particular, L-glutamate which is the crucial precursor in GAD pathway and serves as the hub compound in the carbon and nitrogen metabolism, specifically in nitrogen assimilation in microalgae [34]. In this research, the low level of L-glutamate in *H. pluvialis* demonstrated it has been heavily consumed during the readjustment between carbon metabolism and nitrogen metabolism, coping with the nitrogen-deficient stress. However, significant upregulation of L-aspartate was observed in the LN group, 2.42 fold of the control. The results indicated that the amino acids related to "alanine, aspartate and glutamate metabolism" had the different effects on astaxanthin accumulation and stress response in *H. pluvialis*. Although "lysine biosynthesis" pathway was enriched significantly between the CK and LN group, the content of lysine in the LN group was insignificant compared with the CK group. The results implied that the effects of lysine and "lysine biosynthesis" on astaxanthin accumulation in *H. pluvialis* were not obvious.

As a crucial procedure in the respiratory metabolism, the TCA cycle is considered as not only the hub of carbon-nitrogen metabolism but also the primary energy provider to life activities [42]. The intermediates involved in TCA cycle would provide the carbon skeletons components for the biosynthesis of many vital compounds, including astaxanthin and lipids [43]. In the present research, the contents of the pivotal compounds involved in TCA cycle, including succinate, fumarate and malate, showed a sharp decline in the LN group. The results suggested that TCA cycle was fully activated under the nitrogen constraint stress condition. Furthermore, malate from TCA cycle could

 doi:10.20944/preprints202310.2052.v1

enter into the FA biosynthesis pathway directly through NADP-dependent malic enzyme [44]. And then most of the astaxanthin in *H. pluvialis* was esterified with FA to generate the astaxanthin monoesters and diesters [33]. Therefore, the decline of malate and increase of astaxanthin were observed simultaneously in this study, which demonstrated that the synchronous accumulation of FA and astaxanthin were promoted by the consumption of malate. Furthermore, in order to provide the intermediates and precursors for the recycle of certain amino acids, the upregulation of TCA cycle could be triggered following the massive degradation of protein and amino acid [45]. The view were confirmed by the phenomenon, that the synchronization between sharp decline of most amino acids and significant promotion of TCA cycle in *H. pluvialis* under the nitrogen constraint stress, observed in the present study.

Yet, a series of small molecule organics such as glycolic acid, glyceric acid and formic acid, were supplied by "glyoxylate and dicarboxylate metabolism", with participation in stress resistance and other metabolic pathways. Thus the obvious upregulation of "glyoxylate and dicarboxylate metabolism" pathway was observed in *H. pluvialis* under the nitrogen-deficient stress condition. It was reported that the endogenous nitrogen in *H. pluvialis* would be utilized for crucial amino acids and NAD(P)H production, which supplied the astaxanthin biosynthesis depended on NAD(P)H [26]. In the present study, the level of NADP in the LN group was only 54.21% of the control, which indicated that the biosynthesis of astaxanthin in *H. pluvialis* was activated effectively, leading to a sharp decline of NADP consumed heavily in the process.

4.3. Comparative Analysis of the major carbon metabolism in H. pluvialis under the different stress conditions

According to Figure 9., the patterns of the metabolic features involved in the major carbon metabolism related to the astaxanthin accumulation in *H. pluvialis*, under the high salinity and nitrogen-deficient conditions, varied wildly. Specially, the contents of the metabolites in LN group were almost lower than those both in the CK and HS groups, which indicated that the overall metabolic level stressed by nitrogen-deficient was inhibited, and the astaxanthin was accumulated to response to the stress. This was similar to the previous research [46]. In contrast, the metabolites in HS group were substantially at the higher or close levels contrast to the CK group, which demonstrated the promotion effects of the high salinity on the carbon metabolism related to the astaxanthin accumulation. However, the former study has been shown the reactive oxygen species (ROS) level would increased, accompanied by the astaxanthin accumulation [47].

In fact, the content of astaxanthin accumulated in *H. pluvialis*, meanwhile the level of oxidative stress rised induced by the high salinity unilaterally. The resent research indicated that the transcript levels of the *dxs*, *lcy*, *bkt* and *chy* genes related to the astaxanthin biosynthesis in *H. pluvialis* increased, but the ROS content decreased synchronously under the comprehensive induced conditions containing the high salinity, high-light and endogenous GABA [48]. The results implied that we could use the composite measures to neutralize the side effects of high salinity on the microalgae life actitivies in the astaxanthin production process.

5. Conclusions

In the present study, the differential metabolites and metabolic pathways under the high salinity and nitrogen-deficient stress conditions were highlighted respectively. Furthermore, the metabolic networks related to the astaxanthin accumulation were constucted based on the crucial pathways and metabolites. Moreover, the major carbon metabolism in *H. pluvialis* under the high salinity and nitrogen deficient stress were presented, which exhibited the characteristics in the identified metabolites changes under the different stress conditions.

Author Contributions: Conceptualization, Y.D. and Z.Q.; methodology, Y.D.; software, Y.D.; validation, W.Z.; formal analysis, J.L.; investigation, J.L.; resources, J.L.; data curation, Y.D.; writing—original draft preparation, J.L.; writing—review and editing, Y.D.; visualization, Y.D.; supervision, Z.Q.; project administration, Z.Q.; funding acquisition, Z.Q. All authors have read and agreed to the published version of the manuscript.

Funding: This research was funded by Open Fund of Key Laboratory of Smart Breeding (Co-construction by Ministry and Province), Ministry of Agriculture and Rural Affairs (2023-TJAUKLSBF-2110), Open Fund of Key Laboratory of Marine Ecosystem Dynamics (MED202013) and Tianjin Natural Science Foundation Project (18JCQNJC14800).

Institutional Review Board Statement: Not applicable.

Informed Consent Statement: Not applicable.

Data Availability Statement: All data generated by this study are available in this manuscript.

Conflicts of Interest: The authors declare no conflict of interest and state that the funders had no role in the design of the study; in the collection, analyses, or interpretation of data; in the writing of the manuscript; or in the decision to publish the results.

References

1. Lim, K. C.; Yusoff, F. M.; Shariff, M.; Kamarudin, M. S. Astaxanthin as feed supplement in aquatic animals. *Rev Aquacult*, 2018, 10(3): 738-773.
2. Naguib, Y. Antioxidant activities of astaxanthin and related carotenoids. *J Agr Food Chem*, 2000, 48(4) : 1150-1154.
3. Fang, N.; Wang, C. K.; Liu, X. F.; Zhao, X.; Liu, Y. H.; Liu, X. M.; Du, Y. M.; Zhang, Z. F.; Zhang, H. B. De novo synthesis of astaxanthin: from organisms to genes. *Trends Food Sci Tech*, 2019, 92: 162-171.
4. Wells, L. M.; Potin, P.; Craigie, S. J.; Raven, A. J.; Merchant, S. Sabeeha.; Helliwell, E. K.; Alison, G. S.; Camire, E. M.; Brawley, H. S. Algae as nutritional and functional food sources: revisiting our understanding. *J Appl Phycol*, 2017, 29: 949-982.
5. Tatyana, A. K.; Min, S. K.; Jong, W. H.; Taizo, M.; Chikako, N.; Gwang, H. Kim. Cold-tolerant strain of *Haematococcus pluvialis* (Haematococcaceae, Chlorophyta) from Blomstrandhalvøya (Svalbard). *Algae*, 2013, 28(2): 185-192.
6. He, B. X.; Hou, L. L.; Zhang, F.; Cong, X. M.; Wang, Z. D.; Guo, Y. L.; Shi, J. W.; Jiang, M.; Zhang, X. C.; Zang, X. N.
Ultrastructural changes of *Haematococcus pluvialis* (Chlorophyta) in process of astaxanthin accumulation and cell damage under condition of high light with acetate. *Algae*, 2020, 35(3): 253-262.
7. Mark, A. B.; Ashley, S.; Haley, J.; Richard, P.; Matthew, B. T. The description of *Haematococcus privus* sp. nov. (Chlorophyceae, Chlamydomonadales) from North America. *Algae*, 2023, 38(1): 1-22.
8. Gannoru, K. S. H. N.; Vinoj, C. L.; Pemaththu, H. V. N.; Thilini, U. A.; Chang, J. S. *Haematococcus pluvialis*: A potential feedstock for multiple-product biorefining. *J Clean Prod*, 2022, 344: 131103.
9. Bian, C.; Liu, C. L.; Zhang, G. Y.; Tao, Ming.; Huang, D. Q.; Wang, C. G.; Lou, S. L.; Li, H.; Shi, Q.; Hu, Z. L. A chromosome-level genome assembly for the astaxanthin producing microalga *Haematococcus pluvialis*. *Sci Data*, 2023, 10: 511.
10. Panis, G.; Carreon, J. R. Commercial astaxanthin production derived by green alga *Haematococcus pluvialis*: a microalgae process model and a techno-economic assessment all through production line. *Algal Res*, 2016, 18: 175-190.
11. Shah, R. M.; Liang, Y. M.; Cheng, J. J.; Daroch, M. Astaxanthin-producing green microalga *Haematococcus pluvialis*: from single cell to high value commercial products. *Front Plant Sci*, 2016, 7: 1-28.
12. Zhang, C. H.; Liu, J. G.; Zhang, L. T. Cell cycles and proliferation patterns in *Haematococcus pluvialis*. *Chin J Oceanol Limn*, 2017, 35(5): 1205-1211.
13. Christian, D.; Zhang, J.; Sawdon, J. A.; Peng, C. A. Enhanced astaxanthin accumulation in *Haematococcus pluvialis* using high carbon dioxide concentration and light illumination. *Bioresource Technol*, 2018, 256: 548-551.
14. Liu, Y. H.; Alimujiang, A.; Wang, X.; Luo, S. W.; Balamurugan, S.; Yang, W. D.; Liu, J. S.; Zhang, L.; Li, H. Y. Ethanol induced jasmonate pathway promotes astaxanthin hyperaccumulation in *Haematococcus pluvialis*. *Bioresource Technol*, 2019, 289: 121 720.
15. Li, Y. G.; Cui, D. D.; Zhuo, P. L.; Zhang, L.; Sun, X.; Xu, N. J. A new approach to promote astaxanthin accumulation via Na_2WO_4 in *Haematococcus pluvialis*. *J Oceanol Limnol*, 2019, 37(1): 176-185.
16. Chen, Z.; Chen, J.; Liu, J. H.; Li, L. M.; Qin, S.; Huang, Q. Transcriptomic and metabolic analysis of an astaxanthin-hyperproducing *Haematococcus pluvialis* mutant obtained by low-temperature plasma (LTP) mutagenesis under high light irradiation. *Algal Res*, 2020, 45: 101746.
17. Su, Y. X.; Wang, J. X.; Shi, M. L.; Niu, X. F.; Yu, X. H.; Gao, L. J.; Zhang, X. Q.; Chen, L.; Zhang, W. W. Metabolomic and network analysis of astaxanthin-producing *Haematococcus pluvialis* under various stress conditions. *Bioresource Technol*, 2014, 170: 522-529.

18. Recht, L.; Töpfer, N.; Batushansky, A.; Sikron, N.; Gibon, Y.; Fait, A.; Zarka, A. Metabolite profiling and integrative modeling reveal metabolic constraints for carbon partitioning under nitrogen starvation in the green algae *Haematococcus pluvialis*. *J Biol Chem,* 2014, 289(44): 30387-30403.
19. Lv, H. X.; Xia, F.; Liu, M.; Cui, X. G.; Wahid, F.; Jia, S. R. Metabolomic profiling of the astaxanthin accumulation process induced by high light in *Haematococcus pluvialis*. *Algal Res*, 2016, 20: 35-43.
20. Luo, Q. L.; Bian, C.; Tao, M.; Huang, Y.; Zheng, Y. H.; Lv, Y. Y.; Li, J.; Wang, C. G.; You, X. X.; Jia, B.; Xu, J. M.; Li, J. C.; Li, Z.; Shi, Q.; Hu, Z. L. Genome and transcriptome sequencing of the astaxanthin-producing green microalga, *Haematococcus pluvialis*. *Genome Biol Evol,* 2019, 11(1): 166-173.
21. Dunn, W. B.; Ellis, D. I. Metabolomics: current analytical platforms and methodologies. *Trac-Trend Anal Chem,* 2005, 24(4): 285-294.
22. Shang, M.; Ding, W.; Zhao, Y.; Xu, J. W.; Zhao, P.; Li, T.; Yu, X. Enhanced astaxanthin production from *Haematococcus pluvialis* using butylated hydroxyanisole. *J Biotechnol,* 2016, 236: 199-207.
23. Kokabi, K.; Gorelova, O.; Ismagulova, T.; Itkin, M.; Malitsky, S.; Boussiba, S.; Khozin-Goldberg, I. Metabolomic foundation for differential responses of lipid metabolism to nitrogen and phosphorus deprivation in an arachidonic acid-producing green microalga. *Plant Sci,* 2019, 283: 95-115.
24. Hollywood, K.; Brison, D. R.; Goodacre, R. Metabolomics: current technologies and future trends. *Proteomics*, 2006, 6(17): 4716-4723.
25. Holtin, K.; Kuehnle, M.; Rehbein, J.; Schuler, P.; Nicholson, G.; Albert, K. Determination of astaxanthin and astaxanthin esters in the microalgae *Haematococcus pluvialis* by LC-(APCI) MS and characterization of predominant carotenoid isomers by NMR spectroscopy. *Anal Bioanal Chem,* 2009, 395(6): 1613-1622.
26. Zhang, A. H.; Sun, H.; Wang, P.; Han, Y.; Wang, X. J. Modern analytical techniques in metabolomics analysis. *The Analyst*, 2012, 137(2): 293-300.
27. Boussiba, S.; Fan, L.; Vonshak, A. Enhancement and determination of astaxanthin accumulation in green-alge *Haematococcus pluvialis*. *Method Enzymol,* 1992, 213: 386-391
28. Kanehisa, M.; Araki, M.; Goto, S.; Hattori, M.; Hirakawa, M.; Itoh, M.;, Yamanishi Y. KEGG for linking genomes to life and the environment. *Nucleic Acids Res,* 2007, 36: 480-484.
29. Wang, X. X.; Huang, B. Q.; Zhang, H. Phosphorus deficiency affects multiple macromolecular biosynthesis pathways of *Thalassiosira weissflog* HL. *Acta Oceanol Sin,* 2014, 33(4): 85-91.
30. Ak, B.; Işık, O.; Uslu, L.; Azgın, C. The effect of stress due to nitrogen limitation on lipid content of *Phaeodactylum Tricornutum* (Bohlin) cultured outdoor in photobioreactor. *Turk J Fish Aquat Sci,* 2015, 15: 647-652.
31. Roth, S. M.; Cokus, J. S.; Gallaher, D. S.; Walter, A.; Lopez, D.; Erickson, E.; Endelman, B.; Westcott, D.; Larabell, A. C.; Merchant, S. S.; Pellegrini, M.; Niyogi, K. K. Chromosome-level genome assembly and transcriptome of the green alga *Chromochloris zofingiensis* illuminates astaxanthin production. *PNAS*, 2017, 114(21): 4296-4305.
32. Kobayashi, M.; Sakamoto, Y. Singlet oxygen quenching ability of astaxanthin esters from the green alga *Haematococcus pluvialis*. *Biotechnol Lett,* 1999, 21(4): 265-269.
33. Chen, G. Q.; Wang, B. B.; Han, D. X.; Sommerfeld, M.; Lu, Y. H.; Chen, F.; Hu, Q. Molecular mechanisms of the coordination between astaxanthin and fatty acid biosynthesis in *Haematococcus pluvialis* (Chlorophyceae). *Plant J,* 2015, 81(1): 95-107.
34. Goyal, A. Osmoregulation in Dunaliella, part HL: photosynthesis and starch contribute carbon for glycerol synthesis during a salt stress in *Dunaliella tertiolecta*. *Plant Physiol Bioch,* 2007, 45(9): 705-710.
35. Hoys, C.; Romero-Losada, B. A.; Río, D. E.; Guerrero, G. M.; Romero-Campero, J. F.; García-Gonz´alez, M. Unveiling the underlying molecular basis of astaxanthin accumulation in *Haematococcus* through integrative metabolomic-transcriptomic analysis. *Bioresource Technol,* 2021, 332: 125150.
36. Ding, W.; Cui, J.; Zhao, Y. T.; Han, B. Y.; Li, T.; Zhao, P.; Xu, J. W.; Yu, X. Y. Enhancing *Haematococcus pluvialis* biomass and γ-aminobutyric acid accumulation by two-step cultivation and salt supplementation. *Bioresource Technol,* 2019, 285: 121334.
37. Goiris, K.; Muylaert, K.; Fraeye, I.; Foubert, I.; Brabanter, J.; Cooman, L. Antioxidant potential of microalgae in relation to their phenolic and carotenoid content. *J Appl Phycol,* 2012, 24 (6): 1477-1486.
38. Ding, W.; Li, Q. Q.; Han, B. Y.; Zhao, Y. T.; Geng, S. X.; Ning, D. L.; Ma, T.; Yu, X. Y. Comparative physiological and metabolomic analyses of the hyperaccumulation of astaxanthin and lipids in *Haematococcus pluvialis* upon treatment with butylated hydroxyanisole. *Bioresource Technol,* 2019, 292: 122002.
39. Yu, W. J.; Zhang, L. T.; Zhao, J.; Liu, J. G. Enhancement of astaxanthin accumulation in *Haematococcus pluvialis* by exogenous oxaloacetate combined with nitrogen deficiency. *Bioresource Technol,* 2022, 345: 126484.
40. Chen, H.; Zheng, Y.; Zhan, J.; He, C.; Wang, Q. Comparative metabolic profiling of the lipid-producing green microalga Chlorella reveals that nitrogen and carbon metabolic pathways contribute to lipid metabolism. *Biotechnol Biofuels,* 2017, 10 (1): 153.

41. Zhao, Y.; Yue, C.; Ding, W.; Li, T.; Xu, J. W.; Zhao, P.; Yu, X. Butylated hydroxytoluene induces astaxanthin and lipid production in *Haematococcus pluvialis* under high-light and nitrogen-deficiency conditions. *Bioresource Technol*, 2018, 266: 315-321.
42. Araújo, W. L.; Nunes-Nesi, A.; Nikoloski, Z.; Sweetlove, L. J.; Fernie, A. R. Metabolic control and regulation of the tricarboxylic acid cycle in photosynthetic and heterotrophic plant tissues. *Plant Cell Environ*, 2012, 35 (1): 1–21.
43. Bhosale, P. Environmental and cultural stimulants in the production of carotenoids from microorganisms. *Appl Microbiol Biot*, 2004, 63 (4), 351–361.
44. Bender, S. J.; Durkin, C. A.; Berthiaume, C. T.; Morales, R. L.; Armbrust, E. Transcriptional responses of three model diatoms to nitrate limitation of growth. *Front Mar Sci*, 2014, 1(3): 1-15.
45. Hockin, N. L.; Mock, T.; Mulholland, F.; Kopriva, S.; Malin, G. The response of diatom central carbon metabolism to nitrogen starvation is different from that of green algae and higher plants. *Plant Physiol*, 2012, 158 (1): 299-312.
46. Yong, W. K.; Lim, P. E.; Vello, V.; Sim, K. S.; Abdul, B. M. N.; Mustafa, E. M.; Nik, S. N. M.; Liew, K. E.; Chen, B. J. T.; Phang, S. M. Metabolic and physiological regulation of *Chlorella* sp. (Trebouxiophyceae, Chlorophyta) under nitrogen deprivation. *J Oceanol Limnol*, 2019, 37(1): 186-198.
47. Kobayashi, M. Astaxanthin biosynthesis enhanced by reactive oxygen species in the green alga *Haematococcus pluvialis*. *Biotechnol Bioproc*, 2003, 8 (6): 322.
48. Li, Q. Q.; Zhao, Y. T.; Ding, W.; Han, B. Y.; Geng, S. .; Ning, D. L.; Ma, T.; Yu, X. Y. Gamma-aminobutyric acid facilitates the simultaneous production of biomass, astaxanthin and lipids in *Haematococcus pluvialis* under salinity and high-light stress conditions. *Bioresource Technol*, 2021, 320: 124418.